University of Southern Queensland

School of Engineering

Shear Behaviour of Sandy Clay Infilled Rock Joints

A dissertation submitted by

Jye Barrett

in fulfilment of the requirements of

ENP4111 Professional Engineer Research Project

towards the degree of

Bachelor of Engineering Honours

2024

This page is intentionally left blank

University of Southern Queensland

School of Engineering

ENP4111 Dissertation Project

Limitations of Use

The Council of the University of Southern Queensland, its Academic Affairs, and the staff of the University of Southern Queensland, do not accept any responsibility for the truth, accuracy or completeness of material contained within or associated with this dissertation.

Persons using all or any part of this material do so at their own risk, and not at the risk of the Council of the University of Southern Queensland, its Faculty of Health, Engineering and Science or the staff of the University of Southern Queensland.

This dissertation reports an educational exercise and has no purpose or validity beyond this exercise. The sole purpose of this dissertation project is to contribute to the overall education within the student's chosen degree program. This document, the associated hardware, software, drawings, and other material set out in the associated appendices should not be used for any other purpose: if they are so used, it is entirely at the risk of the user.

CERTIFICATION

I certify that the ideas, designs and experimental work, results, analyses and conclusions set out in this dissertation are entirely my own effort, except where otherwise indicated and acknowledged.

I further certify that the work is original and has not been previously submitted for assessment in any other course or institution, except where specifically stated.

Jye Barrett

Student Number: [redacted]

[redacted] _____

Signature

07/11/2024
_____

Date

ABSTRACT

Understanding the shear behaviour of rock joints is critical to improving the stability and safety of engineering structures, encompassing everything from tunnels to bridges and foundations. Whilst significant research has been conducted previously, further research is required to fully understand and model the shear capacity of rock joints under varying conditions including loadings and infill material properties. In many situations, a significant factor of safety is applied to structures to counteract the unknowns associated with rock joints. Further research and a greater understanding of rock joint shear capacities will allow this factor of safety to be reduced resulting in more economical and sustainable designs.

This project uses direct shear testing machines to investigate the shear behaviour of sandy clay infilled rock joints for a range of normal stress values. Rock samples were created by pouring cement grout into 3D-printed moulds with a triangular asperity. Shear testing was conducted using the ShearTrac2 shear testing machine with varying infill material thicknesses and applied normal stresses. The study tested one infill material type with four thicknesses (0 mm, 1 mm, 2 mm and 3 mm) and 4 loading conditions (150 kPa, 300 kPa, 450 kPa and 600 kPa).

The bulk data was processed using Excel to produce graphical representations of the shear and normal stress against the shear displacement of the joint. The main observation from this project was that the introduction of infill material into the rock joint greatly reduced the maximum shear capacity of the joint. The increase in infill material thickness had little effect on the shear stress of joints with lower applied normal stresses, as the applied normal stress increased the infill material thickness had a greater impact on the shear strength of the rock joint. Overall, the inclusion of material within a rock joint reduces the interaction between the asperities of the joint resulting in lower shear stress values.

ACKNOWLEDGEMENTS

I would like to express my gratitude to my supervisor Dr Ali Mirzaghorbanali for his guidance, feedback and support throughout this project. I am also grateful to the engineering technical staff at the University of Southern Queensland, particularly Wayne Crowell and Heshan Jayasekara, for their invaluable assistance with equipment and troubleshooting, which ensured the smooth progress of experiments and data collection. I extend my sincere thanks to the University of Southern Queensland for providing the facilities and financial support that made this research possible. Finally, I would like to acknowledge my friends and family for their support and patience throughout this project and my studies.

TABLE OF CONTENTS

LIST OF TABLES

LIST OF FIGURES

1 Introduction

1.1 General Introduction

The strength of a rock mass is determined not only by the strength of the rock but also by the shear strength of any discontinuities that exist within it. Current models that aim to determine the shear strength of these discontinuities are inaccurate in many instances. As such, further research is required to produce models that can more accurately determine the shear strength of a large range of rock joints.

1.2 Importance of the Study

Current practice employs engineers to include a large safety factor when designing structures to account for the uncertainties surrounding rock joints. In some instances, this results in unnecessarily over-engineered designs that are uneconomical. With the recent industry focus on sustainable engineering designs and practices, it is more important than ever to ensure that all engineering designs in the future are both sustainable and economical without compromising on safety.

There are three main modes of rock fracture, which are classified by the forces that control it. Type I fractures (the tensile opening mode) are caused by tensile stress acting perpendicular to their surfaces. Type II fractures (the in-plane sliding or shear failures) are subject to shear stress parallel to their surfaces and perpendicular to their leading edges. Type III fractures (tearing or out-of-plane failures) are subjected to shear stress parallel to their surfaces and their leading edges (Li, Zheng, Li, & Zhang, 2024).

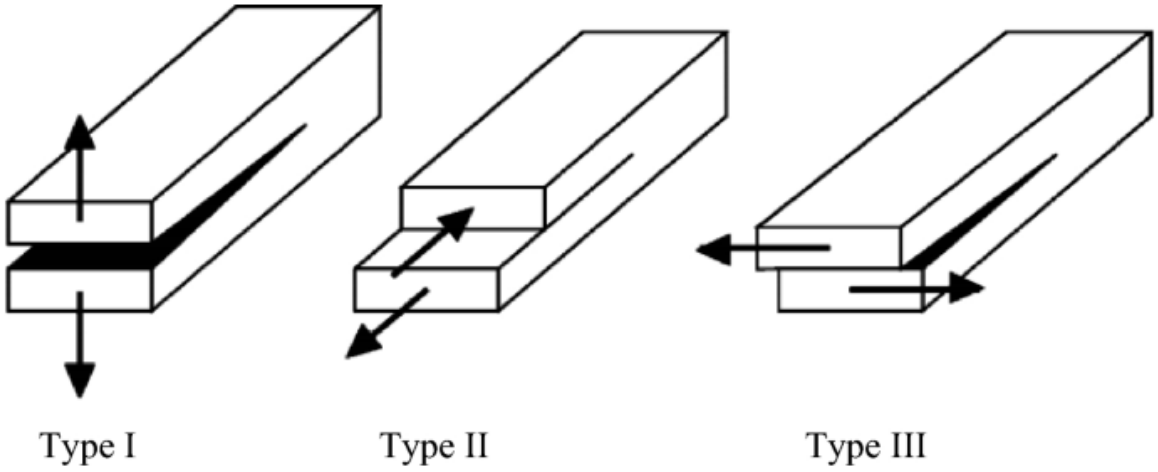

Figure 1 The three types of crack propagation (Li, Zheng, Li, & Zhang, 2024)

One of the most important parameters controlling the shear strength of rock joints is the thickness and properties of infill materials found within the joints. As rock erodes and weathering occurs, fine materials work their way into discontinuities within the rock. The rock joint's strength is influenced by the joint surface's geometry and the infill material's thickness. Many studies have found that the shear strength of the infilled joint decreases as the infill material thickness increases (Jahanian & Sadaghiani, 2014).

1.3 Background to the Study

1.3.1 The Problem

It was outlined above that infill material has a significant impact on the shear strength of rock joints and whilst some research has been conducted in this area, a comprehensive understanding of all infill materials and joint types is yet to be achieved (Zhou, et al., 2022).

As such, this study will further the research on infilled rock joints and endeavour to corroborate findings from past research whilst contributing new research in the future.

To achieve this the project will use a direct shear testing machine to investigate the shear behaviour of sandy clay-infilled rock joints for a range of applied normal stress values and infill material thicknesses. If the project is successful, it will corroborate findings from previous research and contribute new data and findings to the current body of knowledge. Through doing this, further research will be able to call upon findings from this project as well as various other research articles to develop a comprehensive model that is capable of accurately predicting the shear strength of rock joints with a large variety of joint parameters. This will allow engineers to refine structural designs to produce more sustainable and safer structures.

1.3.2 Research Objectives

The main objective of this project is to investigate the shear behaviour of infilled rock joints for a range of normal stress values. The research objectives of this project include:

- A comprehensive literature review of past research in the area of shear strength of both clean and infilled rock joints under both CNL and CNS boundary conditions.
- Identify any gaps in knowledge that are present within current research.
- Develop a research methodology that meets the aims of the investigation for the shear testing of infilled rock joints with a variety of infill thicknesses and normal loadings.
- Execute the research methodology accurately and without bias.
- Accurately record all data available during the testing process.
- Analyse the results of the testing using a graphical representation for shear displacement against shear stress and normal stress for the range of infill materials.

- Discuss the results, draw conclusions and make recommendations on further research.

1.3.3 Outline of the Dissertation

This dissertation consists of 4 chapters followed by a list of references and appendices. The dissertation is organised as follows:

- Chapter 1 outlines the project and introduces the topic.
- Chapter 2 consists of a literature review of previous research on the shear behaviour of rock joints. This chapter aims to establish the existing body of knowledge and identify any gaps that exist within it.
- Chapter 3 develops a methodology for the shear testing of infilled rock joints. This chapter outlines the methods and parameters used when performing the shear tests.
- Chapter 4 presents and analyses the results obtained throughout the testing. The results are presented graphically to aid in the analysis which is then used to draw conclusions and identify any trends that may exist within the results. Finally, this chapter also includes recommendations for further research.

2 Literature Review

2.1 Introduction

Natural rock formations consist of many rock joints, oftentimes these joints are infilled with soil materials which may reduce the shear strength of the rock and affect its stability (Naghadehi, 2015). Depending upon the origin of the rock and the joint, the roughness of the joint may vary from smooth to rough surfaces. Many studies have been performed on smooth joint surfaces with no infill due to their ease of modelling. In practice, these joints are rarely found in natural rock formations prompting further research into infilled rock joints with a larger variety of roughnesses, infill materials, and infill material thicknesses (Shrivatava & Rao, 2017).

2.2 Models for Predicting Shear Strength of Rock Joints

A variety of models have been developed through extensive laboratory testing to try to predict the shear strength of rock joints for a variety of infill materials, infill material thicknesses, and asperity angles under both CNL and CNS loading.

2.2.1 Mechanical Models

One of the first models created for modelling rock joints was by Patton (1966). His model was developed by modelling the shear behaviour of specimens with regular saw tooth-shaped asperities under CNL conditions.

Patton's model was as follows:

Asperity Sliding:

$$\tau_p = \sigma_n \tan(\varphi_b + i_0) \quad [1]$$

Asperity Breakage:

$$\tau_p = \sigma_n \tan(\varphi_b) + c_0 \quad [2]$$

Where τ_p is the peak shear strength of the infilled joint, σ_n is the normal stress corresponding to peak shear stress, φ_b is the basic friction angle in degrees, i_0 is the effective infilled asperity angle in degrees and c_0 is the cohesion.

The model produced by Patton was later modified by Jaeger (1971) to introduce a new failure criterion by replacing the bilinear relationship with a non-linear equation.

Jaeger's model is as follows:

$$\tau_p = \sigma_n \tan(\varphi_b) + (1 - e^{-d\sigma_n})c_0 \quad [3]$$

Where d is an experimentally determined empirical parameter.

Patton and Jaeger's models were both based on rock joints with regular saw tooth-shaped asperities that are rarely found naturally. Barton and colleagues (Barton, 1976) (Barton & Choubey, 1977) proposed a model that incorporates the roughness and irregularity of rock joints using the Joint Roughness Coefficient (JRC). They provided ten standard profiles with JRC values ranging from 0 to 20.

Barton's model is as follows:

$$\tau_p = \sigma_n \tan\left[JRC \log\left(\frac{JCS}{\sigma_n}\right) + \varphi_r\right] \quad [4]$$

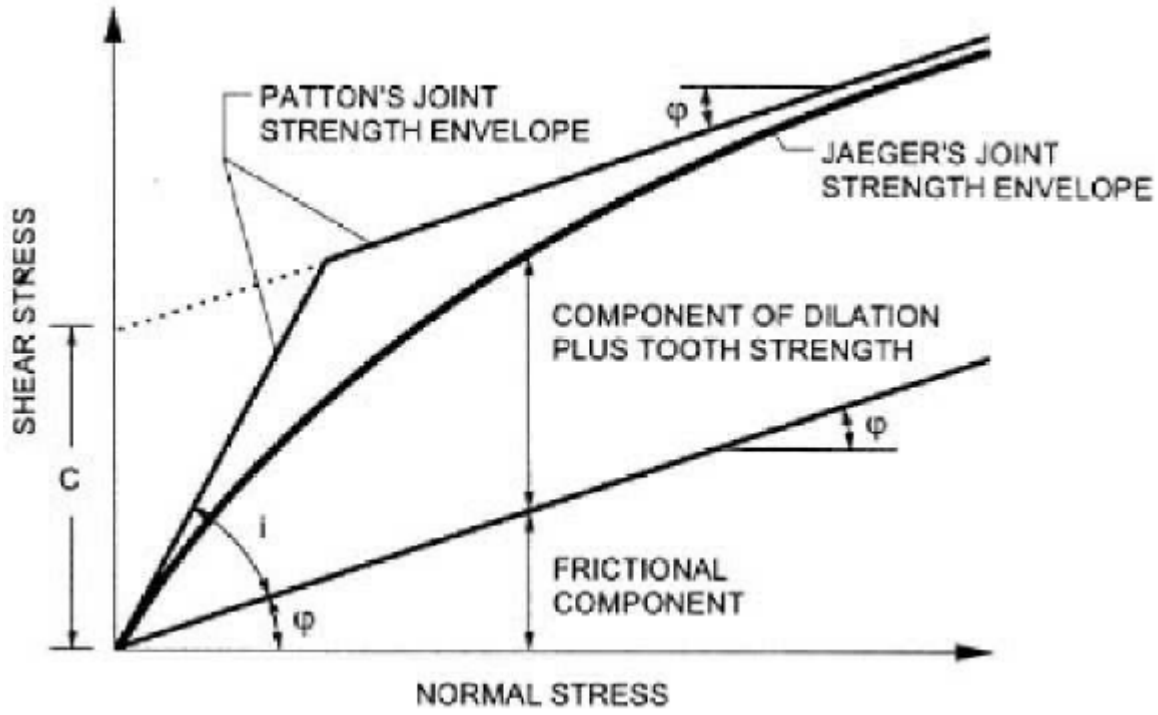

Figure 2 Comparison of rock joint strength components (Vasarhelyi, 1998)

The majority of early testing programs for determining the shear strength of rock joints were performed under CNL boundary conditions. In practice, the shear strength of rock joints is subject to CNS boundary conditions. To conduct testing under CNS conditions Obert, Brady and Schmechel, (1976) and Ooi and Carter, (1987) modified conventional testing used to conduct tests under CNL boundary conditions so that testing could be conducted under CNS boundary conditions. The main limitations of these machines were that it's difficult to change the reaction rods, beams and stiffness plate to simulate different stiffness conditions and whilst changing the stiffness conditions there is a chance that the sample may fail before the start of testing (Shrivatava & Rao, 2017).

To overcome these difficulties and make CNS testing easier and more efficient Jiang, Xiao, Tanabashi and Mizokami, (2004) used servo-controlled equipment to conduct tests. The drawback of this equipment is that it can only be used for relatively small sample sizes making

it difficult to properly study the influence of joint roughness and there is no way of measuring the rotation of the sample. As well as this the equipment can only test samples under normal stiffness conditions ($k_n = 0$) and infinite normal stiffness conditions ($k_n = \infty$) (Shrivatava & Rao, 2017).

There were some limitations to Barton's model, in particular, the estimation of peak shear displacement, post-peak shear strength, dilation and surface degradation. These were described by Asafollahi and Tonon (2010) when they investigated Barton's earlier model. The key finding from the investigation was that the peak shear displacement is independent of the normal stress, although this is not observed during experiments. As well as this they proposed an empirical equation to predict the mobilised JRC, which is used to calculate the shear stress-displacement curve after the peak shear displacement. The equation not only gives a smoother curve when compared to the linear interpolation of the values given in Barton's table but is also easier to implement numerically. They also proposed equations to obtain the pre and post-peak dilation for each shear displacement that doesn't contain the inconsistencies found in Barton's model. Finally, they introduced a table to simulate the pre-peak shear stress-displacement curve that gives the mobilised JRC and base friction angle at each shear displacement (Asadollahi & Tonon, 2010).

2.2.2 Mathematical Models

One of the earliest mathematical models proposed to determine the shear stress of rock joints under CNL conditions was produced by Heuze (1979). Heuze's model emphasised that when a joint dilates it is restrained by external normal stiffness across the rock joint that increases the normal stress. He used an analytical method to calculate the incremental normal stress as a function of external boundary stiffness (Thirukumaran & Indraratna, 2016).

In Heuze's model the incremental normal stress ($\Delta\sigma_n$) is formed by a positive dilation $\Delta\delta_V$ that compresses the constant stiffness of a spring. The joint is prevented from opening due to the normal stiffness of the joint (Thirukumaran & Indraratna, 2016). The equation used to express the equilibrium of $\Delta\delta_V$ is shown below:

$$d\delta_V = \frac{\partial\delta_V}{\partial\delta_h} d\delta_h + \frac{\partial\delta_V}{\partial\sigma_n} d\sigma_n \quad [5]$$

Where $\frac{\partial\delta_V}{\partial\delta_h} = \tan i$ and $\frac{\partial\delta_V}{\partial\sigma_n} = \frac{-1}{k_n}$

The equation proposed by Heuze (1979) to calculate the increment of normal stress under CNS conditions was as follows:

$$d\sigma_n = \tan i \left(\frac{k_n K_n}{k_n + K_n}\right) d\delta_h \quad [6]$$

Where $d\delta_h$ is the shear displacement.

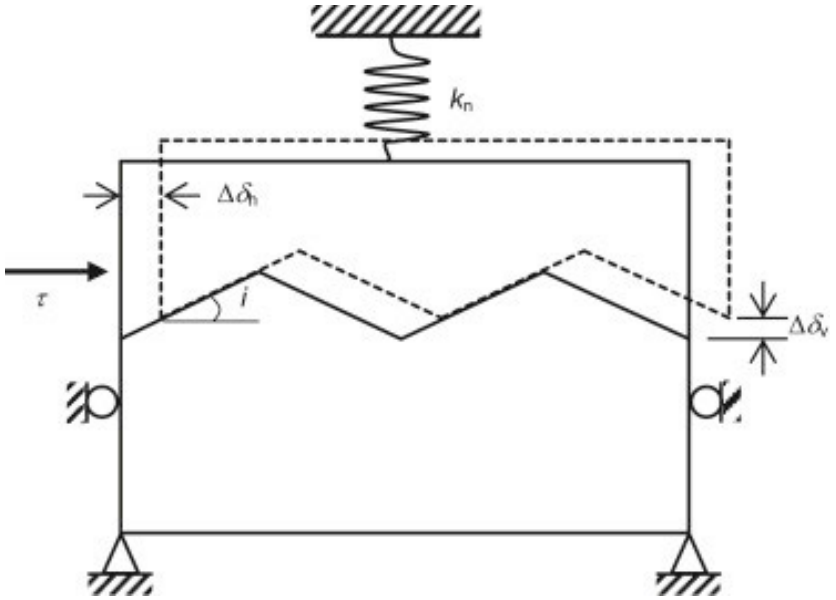

Figure 3 Conceptual model of dilatant joints using Heuze (1979) model (Thirukumaran & Indraratna, 2016).

Heuze (1979) described a three-degree polynomial equation to model the peak shear strength of a rock joint below the critical normal stress. The following can be used to determine the peak shear stress $(\tau_p)_{CNS}$:

$$(\tau_p)_{CNS} = a\sigma_n + b{\sigma^2}_n + c{\sigma^3}_n \quad [7]$$

Where $a = \tan\phi_p$, $b = \frac{3C_p}{{\sigma^2}_{cr}} - \frac{2(\tan\phi_p - \tan\phi_r)}{\sigma_{cr}}$ and $c = -\frac{2C_p}{{\sigma^3}_{cr}} + \frac{2(\tan\phi_p - \tan\phi_r)}{{\sigma^2}_{cr}}$

Where σ_n is the normal stress, σ_{cr} is the critical normal stress, $C_p$is the apparent cohesion, ϕ_p is the peak friction angle and ϕ_r is the residual friction angle (Thirukumaran & Indraratna, 2016).

Leichnitz (1985) used the results obtained from CNS and CNL testing to show that the shear force (S) and normal displacement (v) are independent of a given stress path. It was found that they are the functions of the shear displacement (u) and normal force (N) rather than the stiffness. He was able to propose partial differential equations as follows to predict the shear response under CNS boundary conditions (Thirukumaran & Indraratna, 2016):

$$dS = \frac{\partial \hat{S}}{\partial u}du + \frac{\partial \hat{S}}{\partial N}dN \quad [8]$$

$$dv = \frac{\partial \hat{v}}{\partial u}du + \frac{\partial \hat{v}}{\partial N}dN \quad [9]$$

Based on a graphical analysis by Saeb and Amadai (1990), Saeb and Amadai (1992) proposed in a later study that the total normal displacement of a joint (v) must be a function of the shear displacement (u) and the normal stress (σ_n) (Thirukumaran & Indraratna, 2016). The following equation describes this relationship:

$$v = u\left(1 - \frac{\sigma_n}{\sigma_T}\right)^{k_2} \tan i_0 + \frac{\sigma_n V_m}{k_{ni} V_m - \sigma_n} \quad [10]$$

Where σ_T is the transitional stress which is obtained from experimental results, i_0 is the initial dilation angle, k_2 is the empirical constant with a value of 4 as determined by Landanyi and Archambault (1970), V_m is the maximum joint closure and k_{ni} is the initial normal stiffness (Thirukumaran & Indraratna, 2016).

By differentiating and rearranging the above you get the following equation:

$$d\sigma_n = \frac{dv - \left(1 - \frac{\sigma_n}{\sigma_T}\right)^{k_2} \tan i_0 \, du}{-\frac{uk_2}{\sigma_T}\left(1 - \frac{\sigma_n}{\sigma_T}\right)^{k_2 - 1} \tan i_0 + \frac{k_{ni} V^2{}_m}{(k_{ni} V_m - \sigma_n)^2}} \quad [11]$$

This can be rewritten as follows:

$$d\sigma_n = k_{nn} dv + k_{nt} du \quad [12]$$

Where $k_{nn} = \frac{\partial \sigma_n}{\partial v}$ and $k_{nt} = \frac{\partial \sigma_n}{\partial u}$. Although this simplified equation only applies when $\frac{\sigma_n}{\sigma_T} < 1$ (Thirukumaran & Indraratna, 2016).

Saeb and Amadai (1992) also proposed an equation that represents the shear stress as follows:

$$d\tau = k_{tn} dv + k_{tt} du \quad [13]$$

Where $k_{tn} = \frac{\partial \tau}{\partial v}$ and $k_{tt} = \frac{\partial \tau}{\partial u}$.

Saeb and Amadai (1992) used two models that were recommended by Goodman (1976) to represent the joint shear stress to shear displacement behaviour under CNL boundary conditions (Thirukumaran & Indraratna, 2016). These are shown below:

$$\left.\begin{aligned}\tau &= k_s u \\ k_s &= \frac{\tau_p}{u_p}\end{aligned}\right\}\left(u < u_p\right) \qquad [14]$$

$$\tau = \frac{\tau_p - \tau_r}{u_p - u_r}u + \frac{\tau_r u_p - \tau_p u_r}{u_p - u_r}\left(u_p \le u < u_r\right) \qquad [15]$$

$$\tau = \tau_r (u > u_r) \qquad [16]$$

Where τ_p is the peak shear stress, τ_r is the residual shear stress, u_p is the peak shear displacement and u_r is the residual shear displacement (Thirukumaran & Indraratna, 2016).

A visco-plastic multi-laminate model for the shear behaviour of rock joints under CNL conditions was produced by Roosta, Sadaghaiana, Pak & Saleh (2006). The model is based on the Mohr-Coulomb failure criterion. The yield functions in shear and tension at joints are defined as:

$$F_s = \tau + \sigma_n \tan(\phi_m) - c_m \qquad [17]$$

$$F_t = \sigma_n - \sigma^t \qquad [18]$$

Where, σ^t is the tensile strength of rock joints, c_m is mobilised cohesion and ϕ_m is mobilised friction angle.

Increasing or decreasing the mobilised cohesion or friction angle with plastic shear displacement leads to the hardening or softening phenomenon. The following model is proposed for the mobilised friction angle:

$$\phi_m = \frac{\sqrt[2]{u^P \times u_p^P}}{u^P + u_p^P}\left(\sin\phi_p - \sin\phi_0\right) + \sin\phi_0 \qquad u \le u_p \qquad [19]$$

Where u^P is plastic shear displacement, u_p^P is the plastic shear displacement at the peak friction angle ϕ_p, and ϕ_0 is the initial friction angle.

A linear relationship was proposed for the softening part to define the mobilised friction angle from the peak friction angle to the residual friction angle. Mobilised cohesion and tangent of mobilised dilation angle are given by the following:

$$c_m = c_0 \exp(-\lambda u^P) \quad [20]$$

$$\tan(\psi_m) = \alpha u^P + \beta \quad [21]$$

Where, c_0 is the initial cohesion, λ is the rate of reduction in cohesion and α and β are parameters depending on the normal stress and joint roughness (Roosta, Sadaghaiana, Pak, & Saleh, 2006).

2.2.3 Graphical Models

It was noted by Seab and Amadei (1990) that a constant or variable boundary condition is more likely to exist rather than CNL conditions for joints in situ. As such they extended Goodman's (1980) graphical model to predict the shear behaviour of rough joints under constant or variable normal stiffness conditions. This was achieved by coupling the closure of joints at different shear displacements and shear behaviours under CNL boundary conditions.

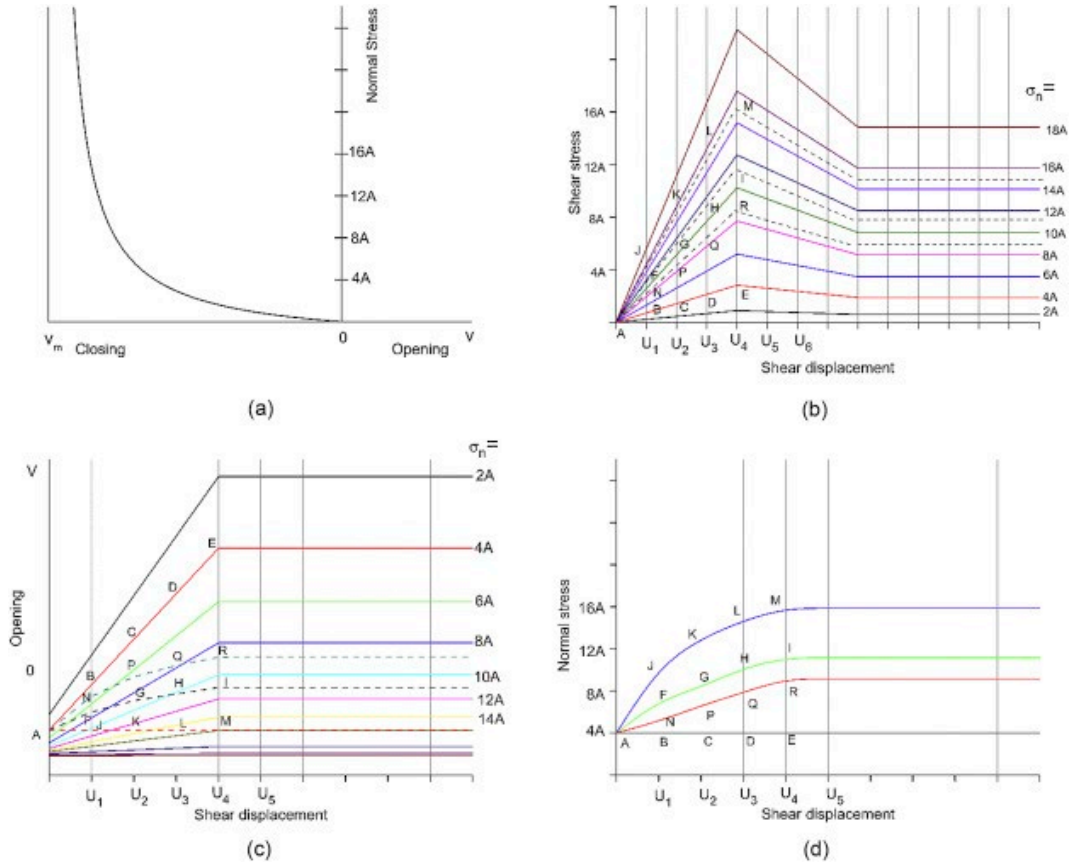

Figure 4 Joint response curves for normal stress ranging between 0 and 20A (after Saeb & Amadei, 1990)

From Figure 4 above it can be seen that the curve $u = u_0$, representing the joint under mated conditions is the same as the joint closure against a normal stress curve (Figure 4a). Also, each curve $u = u_i$ represents the behaviour of the rock joint under normal loading after being mismatched by a shear displacement (u_i). It can also be seen that there is no dilation for values of u greater than u_4 (Figure 4c). As such the joint response is admissible if it is within the domain of the curves $u = u_0$ and $u = u_4$. All curves $u = u_i$ $(i = 1,4)$ become closer to the curve $u = u_0$ due to the joint dilation decreasing as the normal stress increases.

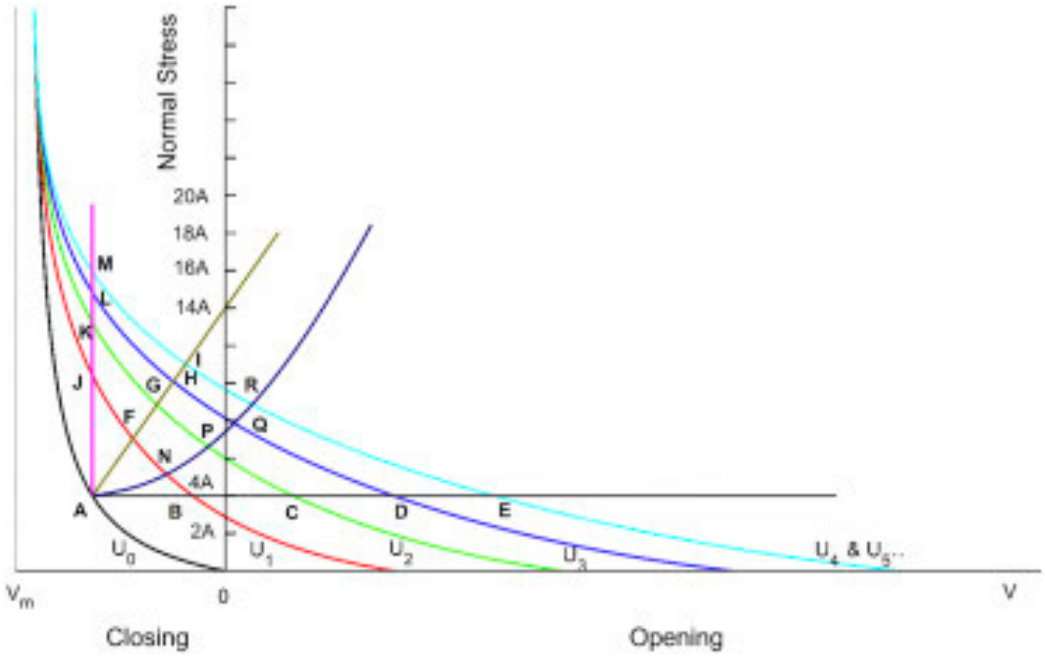

Figure 5 Normal stress versus normal displacement curves at different shear displacement levels (after Saeb & Amadei, 1990).

The shear strength of rock joints for any load path can be estimated using Figures 4 and 5. Figure 5 shows four distinct load paths that originate from point A, assuming that a normal stress $\sigma_n = 4A$ was first applied before shearing. The joint follows the path $AFGHI$ under CNS conditions (k_n), under CNL conditions ($k_n = 0$) it would follow the path $ABCDE$ and when no change in the joint normal displacement is allowed ($k_n = \infty$). The final path $ANPQR$ corresponds to a joint in a rock mass with increasing applied normal stiffness.

In Figure 5, by recording the values of σ_n and u at the point of intersection of each path with curves u_i and using Figures 4b and c, the shear stress against shear displacement for normal stress equal to $4A$ can be found, as indicated by the dashed lines.

2.3 Infill Material

A major influence towards the shear strength of a rock joint is the presence of infill material, with the thickness and type of material having significant effects on the joint shear strength. Brekke and Howard (1972) proposed seven groups of rock joints based on infill materials according to their strength and behaviour:

1. Healed or “welded” discontinuities.
2. Clean discontinuities, i.e., closed but without filling or coatings.
3. Calcite fillings.
4. Coatings or fillings of chlorite, talc and graphite.
5. Inactive clay material.
6. Swelling clay.
7. Material that has been altered to a more cohesionless (sand-like) material.

Ladanyi and Archambault (1977) then divided infill material types found in rock joints into four groups:

1. Clean, i.e., non-filled or without coating.
2. Coated.
3. Clay-like infilling.
4. Sand-like infilling.

Lama (1978) categorised the filling material that exists within the interfaces into the following groups based on the material origin and the method of transport:

1. Loose material brought from the surface such as sand, or clay.
2. Deposition by groundwater flow containing products of leaching of calcareous of ferruginous rocks.

3. Loose material from tectonically crushed rock.
4. Products of decomposition and weathering of joints.

2.4 Shear Rate

Crawford and Curran (1981) offer an in-depth investigation into the effect of shear rate on the shear behaviour of soft and hard rock joints. The main focus of their work was the relationship between shear displacement rates, joint surface morphology and the resulting shear strength. They conducted shear tests under CNL conditions with shear rates of 0.05-50 mm/s with a normal stress ranging from 0.62 MPa to 2.78 MPa.

The study found that at higher shear rates the asperity is more likely to crush with an increase in surface wear as well. However, the tests found that hard and soft rocks are influenced differently by the rate of shearing. Generally, the hard rock specimens showed a decrease in shear strength with an increase in shear rate. Conversely, for softer rock joints, the frictional resistance increases to a critical shear displacement and then remains unaffected by further increases in shear rate (Crawford & Curran, 1981).

The results obtained by Crawford and Curran were verified by Jafari, Pellet, Boulon and Hosseini (2004) for shear rates between 0.05 mm/min and 0.4 mm/min for harder rock joints.

Indraratna and Haque (1999) studied the shear strength of soft rock joints under CNS conditions with a variety of shear rates ranging from 0.35 mm/min to 1.67 mm/min. The tests had a normal stress of 0.56 MPa and an asperity angle of 18.5^{o}. These tests showed that for soft rock joints the peak shear strength increases along with the shear rate (Indraratna, Haque, & Aziz, 1999).

3 Methodology

3.1 Mould Design

Rock specimens are to be created using moulds from the previous research project 'Shear strength properties of clean and clay infilled rock joints: an analysis of the impact of moisture content under CNL conditions' (Downing, Mirzaghorbanali, & Aziz, 2023). The moulds required a diameter of 63 mm and an overall height of 36 mm to fit in the ShearTrac2 testing machine. The diameter of the base plate determined the internal diameter of the casting moulds, and the overall height includes both the top and bottom interlocking cement grout joints as well as the infill material thickness. (Downing, Mirzaghorbanali, & Aziz, 2023).

A single uniform sawtooth asperity profile was used with an asperity height of 2 mm, asperity length of 7 mm and an asperity angle of 29.7°. The mould was printed using an Anycubic Mono X (4K) SLA printer with Anycubic's standard grey UV resin with a layer height of 50 microns (Downing, Mirzaghorbanali, & Aziz, 2023).

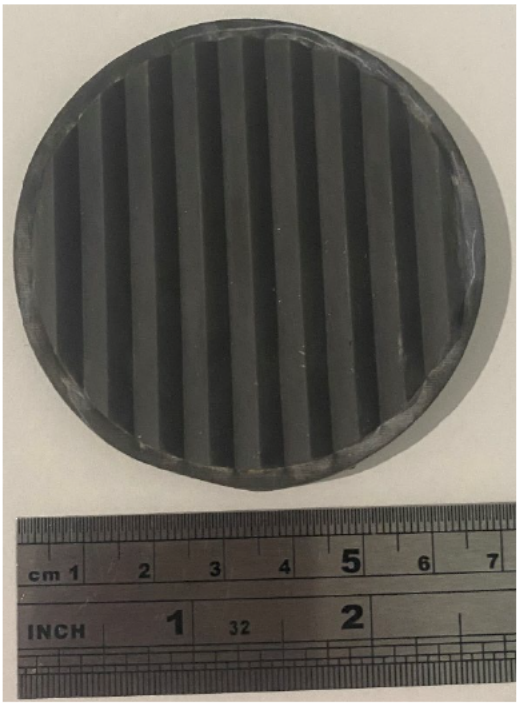

Figure 6 Top view of mould base

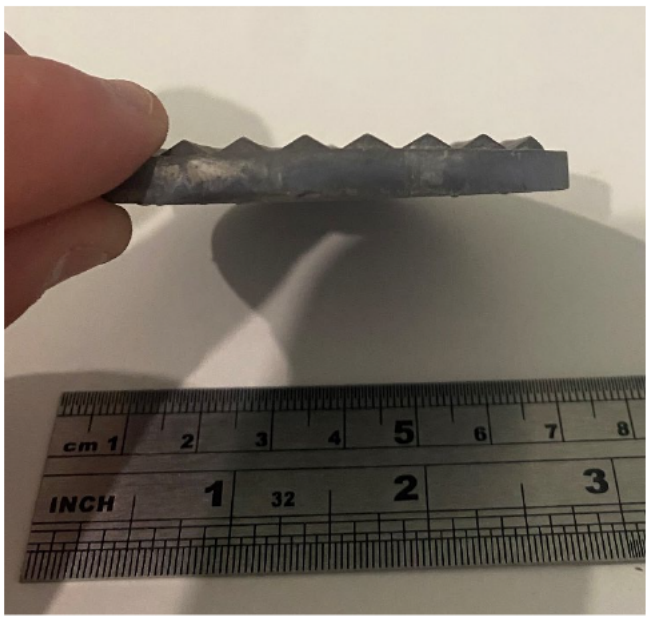

Figure 7 Side view of mould base

3.2 Mould Preparation

The moulds were cleaned using a hard bristled brush to remove any cement grout residue left from past experiments to ensure the sawtooth profile was unobstructed. PVC pipe was cut to a length of 20 mm and fixed to the base to create a cylindrical mould. The PVC pipe was fixed to the base using masking tape to ensure a secure bond and prevent any grout from spilling out from the mould when casting.

To aid in the release of the mould from the specimen after curing, the PVC pipe was split vertically in one place and the inside of the mould was coated with oil to prevent the cement grout from adhering to the mould. Care was taken when applying oil to the inside of the mould to preserve the sawtooth profile.

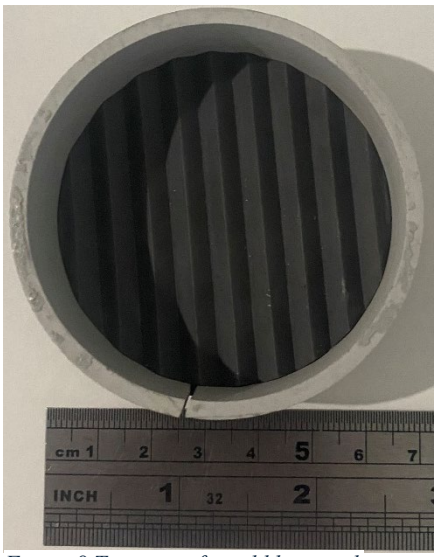

Figure 8 Top view of mould base with PVC extrusion

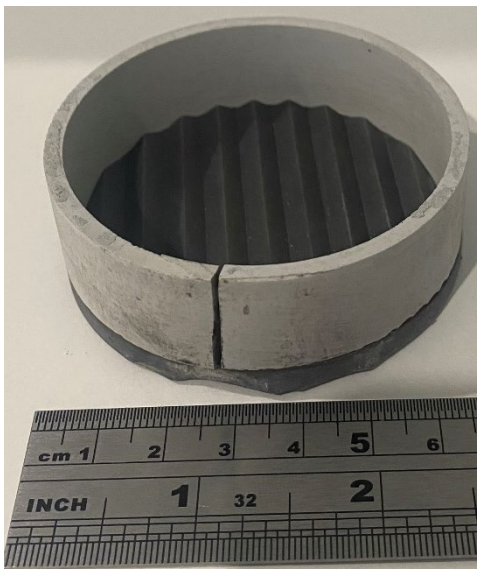

Figure 9 Side view of mould with PVC extrusion

Figure 10 Taped moulds with oil applied

In addition to the rock specimens, 3 cubic moulds with dimensions of 50 mm were also cast. Again, the inside of the moulds was coated with oil to ensure the specimens could be removed easily after they had cured. These cubes were used to verify the compressive strength of the concrete mixture.

3.3 Casting Process

The moulds were filled with a custom mix of flowable cement grout. A ratio of 1kg of Portland cement, 3kg of fine sand and 800mL of water was used for the grout mix. The grout mixture was then poured into the sawtooth moulds ensuring that the mixture was agitated to release any trapped air bubbles, and the sawtooth profile was moulded fully. As well as pouring the grout into the sawtooth moulds the mixture was also poured into the cubic moulds. Again, the moulds were agitated to ensure all air bubbles were released and the mixture filled the mould completely. Care was taken to ensure that the top of the concrete was finished with a flat surface with no voids or uneven sections. This ensured that the mould sat correctly within the ShearTrac2 testing machine. The grout was allowed to cure for 48 hours before being demoulded. After removal, the moulds were marked to indicate the top and bottom sections of each joint. The specimens were then cured for 10 days.

Figure 12 Cement grout mixture

Figure 11 Grout-filled sawtooth moulds

Figure 13 Grout-filled cubic moulds

Figure 14 Cured concrete samples

3.4 Compressive Strength Testing

The uniaxial compressive strength of the cement grout was measured to determine the rock type and properties of the moulds. The 50 mm cubes, that were cast along with the sawtooth moulds, were placed into the uniaxial compressive testing machine. A loading rate of 0.5 kN/s was used, and the peak compressive strength of the sample was recorded. The samples were tested after 10 days with 3 tests performed to find the average compressive strength of the grout mix.

The three samples tested returned maximum compressive strength values of 3.577 MPa, 1.836 MPa and 2.269 MPa. The average compressive strength of the cement grout was 2.56 MPa. The rock sample is classified as a soft rock as the average compressive strength is less than 20 MPa. In particular, the sample has strength values similar to that of sandstone (Agustawijaya, 2007).

Figure 15 Cubic moulds after compression testing

3.5 Infill Material

The infill material was selected to simulate sandy clay material found naturally in many rock joints. It was a mixture of fine sand and bentonite clay at a ratio of 40% sand, 50% clay and 10% water by weight.

The infill material was then tested to determine its moisture content. Three samples were oven-dried over 24 hours to determine their moisture content in accordance with the AS1289.2.1.1-2005 Method of testing soils for engineering purposes. The average moisture content of the infill material was 63.1%

3.6 Infill Material Thickness

One of the independent variables being tested in this project is the infill material thickness to asperity height ratio (t/a). As the rock joint samples had only one asperity height the thickness of the infill material was changed throughout the tests. Four infill material thicknesses were tested for each loading condition. Thicknesses of 0 mm (clean joint), 1 mm, 2 mm and 3 mm were used. This resulted in t/a of 0, 0.5, 1, 1.5 respectively.

3.7 Loading Conditions

The other independent variable being tested in this study is the normal stress values used within the direct shear testing machine. Four normal loading conditions of 150 kPa, 300 kPa, 450 kPa and 600 kPa were used during the direct shear testing of the specimens. This resulted in a total of 16 shear test specimens.

3.8 Direct Shear Testing

A total of 16 direct shear tests were conducted using a direct shear testing machine under CNL conditions. Firstly, the bottom cast rock joint profile was placed into the bottom of the shear box on top of the metal plate. Then, the required thickness of infill material was placed onto the top of the sample. Following this, the top half of the shear box was placed over the mould and the top sample was placed on top of the infill material, taking care to ensure that the asperities of the two cast sections lined up within the shear box and perpendicular to the horizontal movement axis of the machine. Two plastic bolts were used to fix the top and bottom sections of the shear box, and the shear box was placed within the ShearTrac2 machine.

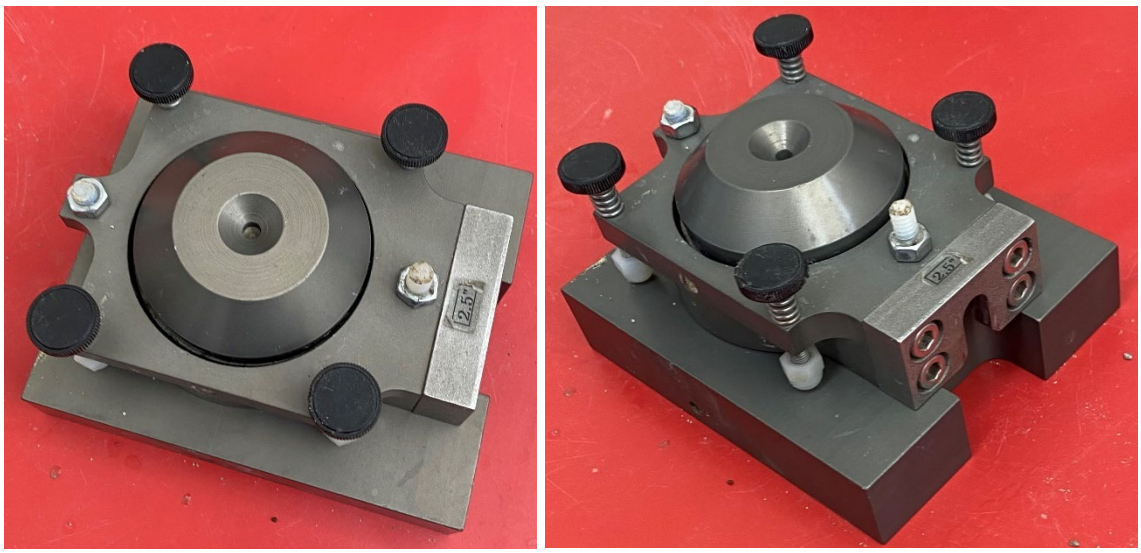

Figure 16 Shear box with a sample inside before being placed in ShearTrac2 machine

The horizontal and vertical axis of the ShearTrac2 machine were then initialized. After this, the top metal plate was placed on top of the mould with a small metal ball placed atop it. The horizontal bar was lowered, and the strain gauge was placed on top of the metal ball.

Figure 17 ShearTrac2 shear testing machine

After the mould had been placed correctly within the ShearTrac2 machine the computer was used to load the Shear Test Template and define the parameters for the test being conducted. After the initial consolidation period had been completed the two plastic bolts were removed and the shear test was completed. Due to the limitations of the machine, the test was aborted if a maximum of 20 mm horizontal movement or 2200N shear load was reached.

After the test had been completed the results files were saved to the computer and the sample was removed from the ShearTrac2 machine. The next sample was prepared and placed into the machine as described above.

3.9 Recording Results

In order to organise results and easily identify the variables of each one, a code was allocated to each test. The code consists of two digits, the first indicates the loading condition of the specimen, numbered 0-3 correlating with loadings of 150 kPa, 300 kPa, 450 kPa and 600 kPa respectively. Likewise, the second number represents the infill material thickness, numbered 1-4 correlating with infill thicknesses of 0 mm, 1 mm, 2 mm and 3 mm.

Table 1 Testing Parameters

Specimen Code	Loading (kPa)	Infill Thickness (mm)	T/A Ratio
01	150	0.0	0.0
02	150	1.0	0.5
03	150	2.0	1.0
04	150	3.0	1.5
11	300	0.0	0.0
12	300	1.0	0.5
13	300	2.0	1.0
14	300	3.0	1.5
21	450	0.0	0.0
22	450	1.0	0.5
23	450	2.0	1.0
24	450	3.0	1.5
31	600	0.0	0.0
32	600	1.0	0.5
33	600	2.0	1.0
34	600	3.0	1.5

4 Results and Discussion

4.1 Shear Displacement vs Shear Stress

This section presents the graphical summaries of the results from the direct shear testing of both clean and infilled rock joints regarding the shear displacement and shear stress variables. The data was collected as outlined above in the methodology with the bulk data processed using Excel.

4.1.1 Clean Joints with a normal stress of 150 kPa, 300 kPa, 450 kPa and 600 kPa

Figure 18 shows a comparison of clean rock joints (T/A = 0) with applied normal stress of 150 kPa, 300 kPa, 450 kPa and 600 kPa. When a normal stress of 600 kPa was applied, the test was aborted before 3mm of horizontal displacement was achieved as the ShearTrac2 machine exceeded the maximum allowable shear stress limit of 2200 N.

All the tests with clean joints showed a significant initial rise in the shear stress to a maximum value. After the initial peak, the shear stress reduced significantly and formed a wave pattern, where the variance in shear stress was relatively small for the remainder of the test. The loading that showed the greatest variance in shear stress after the initial peak was the test with a normal stress of 300 kPa. The test with a normal stress of 150 kPa didn't show a large initial increase in shear stress and showed little variance in shear stress throughout the test. This is likely because the normal stress applied wasn't large enough to cause considerable shear resistance as the two rock samples moved past each other with the asperities being able to slide over each other with minimal force variation. In contrast, the sample with a normal force of 450 kPa

showed a significant initial increase in shear stress at approximately 2.5 mm of shear displacement followed by a large decrease with little variation in the shear stress experienced after this. The initial increase in shear stress is likely due to the normal stress not allowing the asperities to slide past each other and as a result is caused by the asperities of the joints breaking. After the asperities had sheared off there was minimal variation in the shear stress, as the joint surface had flattened. This same trend is likely to have been observed in the 600 kPa sample with an initial spike in shear stress as the protrusions of the joints broke followed by a decrease in shear stress and little variation for the remainder of the test. The test with a normal stress of 300 kPa experienced a significant initial increase in shear stress similar to the 450 kPa test. Unlike the 450 kPa test, following the initial spike in shear stress a wave profile was created with a wavelength of approximately 7 mm. Similar to the 150 kPa test, the lower normal stress likely allowed the two samples to slide over each other after a small portion of the asperity was broken off the top of the joints. As the asperity wasn't broken perfectly flat, the shear stress increased as the high points of the asperity passed each other resulting in the wave pattern.

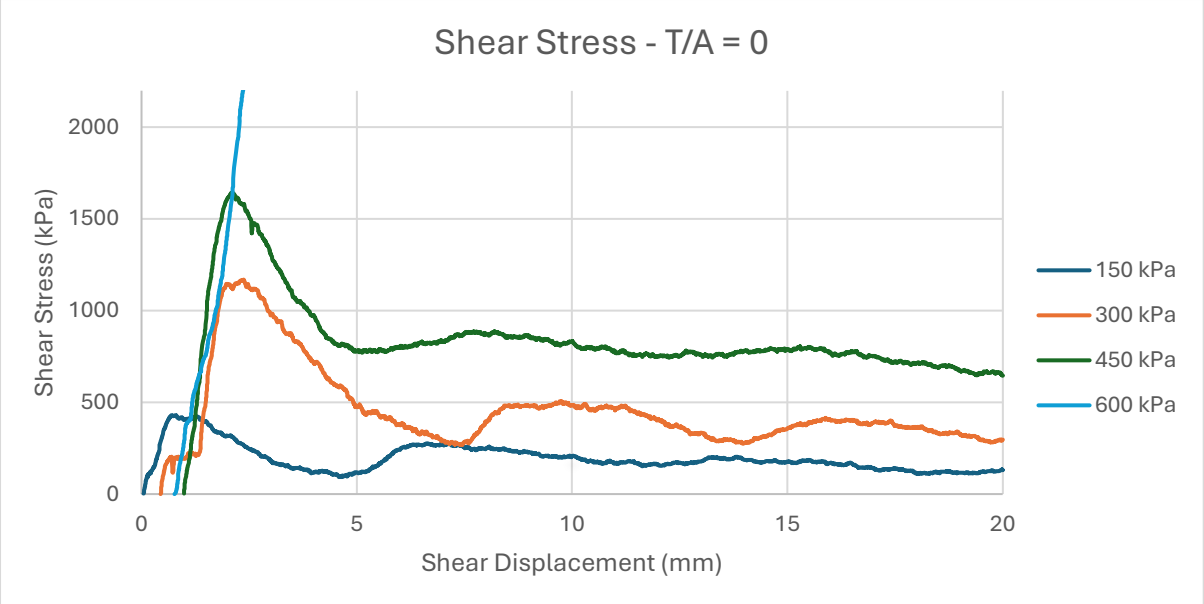

Figure 18 Shear testing results for clean joints (T/A = 0) (Shear Displacement vs Shear Stress)

4.1.2 Infilled Joints with a Thickness of 1 mm (T/A = 0.5)

Figure 19 shows a comparison of rock joints with an infill thickness of 1 mm (T/A = 0.5) with applied normal stress of 150 kPa, 300 kPa, 450 kPa and 600 kPa. The maximum shear stress value of all the tests is significantly less than the shear stress values for clean joints with the same loading. Similar to the clean joints, the shear stress increased substantially at the start of the test, although, unlike the tests with clean joints, the shear stress didn't see any significant decrease from the initial value for most of the loading conditions. The test with a normal stress of 450 kPa was the only test to show a reduction in shear stress after the initial peak. This test also showed the wave profile seen in the clean joint tests. The other tests had a relatively consistent shear stress value after the initial increase at the beginning of the test. This shows that the inclusion of infill material in the rock joint not only reduces the joint's shear resistance but also minimizes the effect of the asperity profile on the shear strength of the joint.

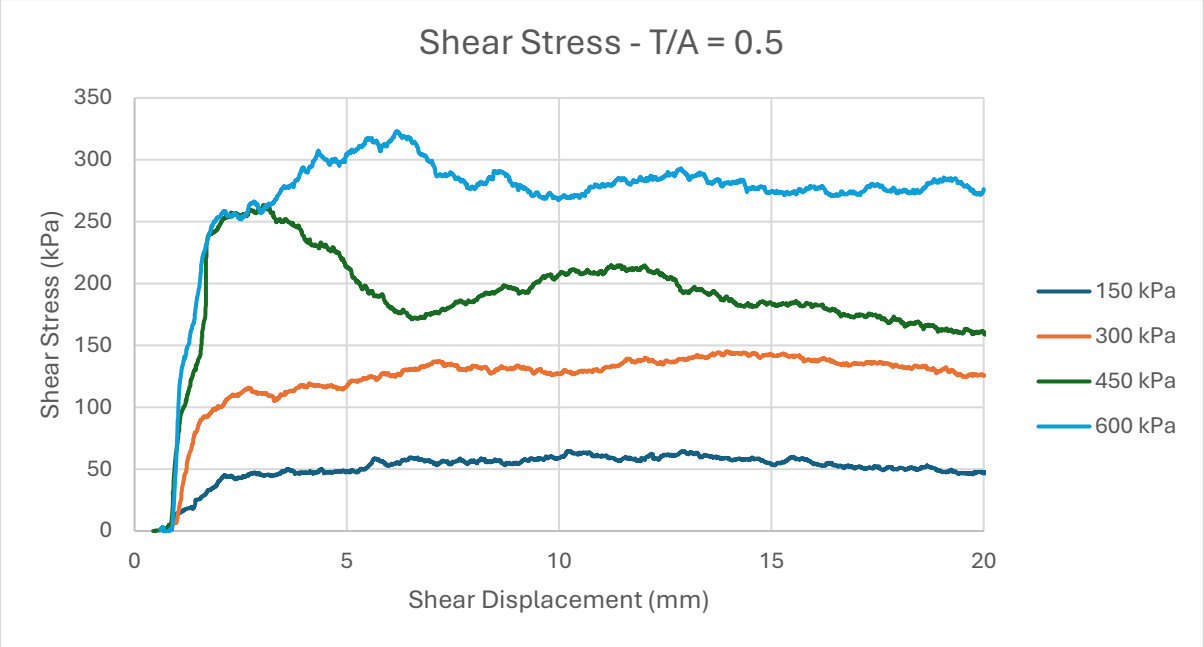

Figure 19 Shear testing results T/A = 0.5 (1 mm) (Shear Displacement vs Shear Stress)

4.1.3 Infilled Joints with a Thickness of 2 mm (T/A = 1)

Figure 20 shows a comparison of rock joints with an infill thickness of 2 mm (T/A = 1) with applied normal stress of 150 kPa, 300 kPa, 450 kPa and 600 kPa. The maximum shear stress values in the tests are lower than in tests with an infill thickness of 1mm. However, the reduction in shear stress is significantly smaller compared to the decrease observed when comparing clean joints to joints with 1 mm of infill material. The test with a normal stress value of 150 kPa shows a gradual rise in shear stress whereas the other tests show an initial, more abrupt increase in shear stress. Following this, the test with a normal stress value of 600 kPa shows a wave profile, again with a wavelength approximately equal to the asperity length of the joint. The tests with a normal stress value of 300 and 450 kPa show less variation in the shear stress as the samples move, with the shear stress gradually increasing as the displacement increases. This is unlike the shear stress values observed in the tests with a clean joint, as the shear stress values began to decrease as the displacement of the samples increased. As was observed for the tests with 1 mm of infill material the increase in infill material thickness results in a lower shear resistance throughout the joint and minimised the effect of the asperity profile of the joint on the shear resistance.

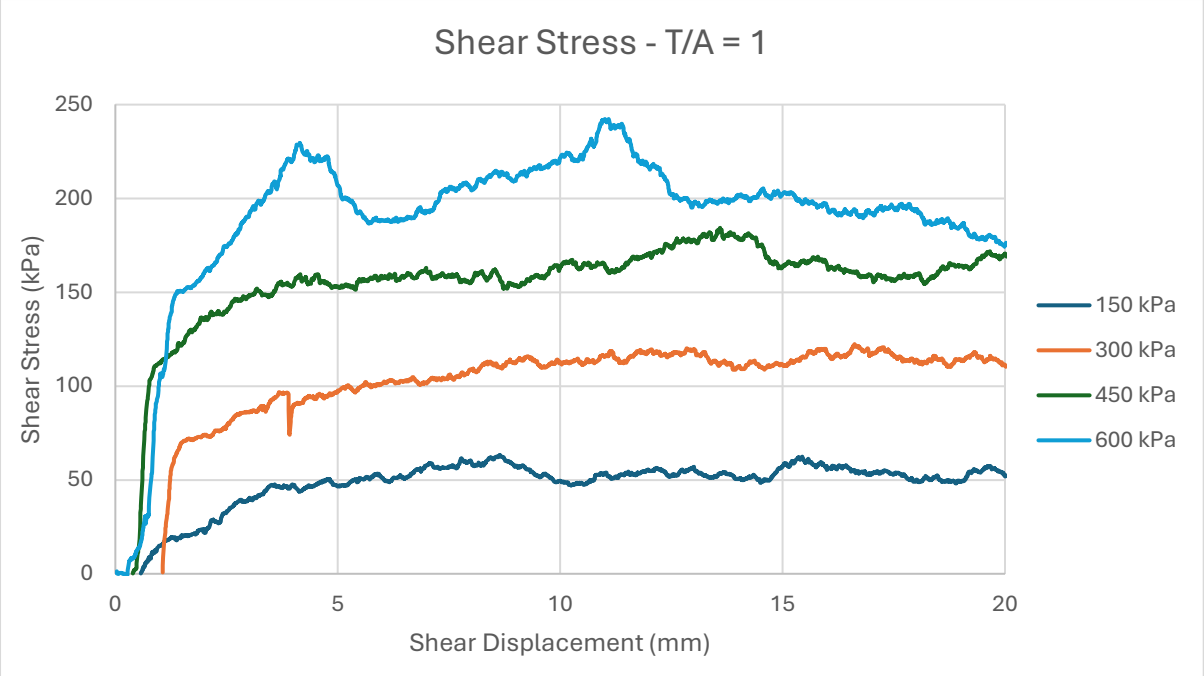

Figure 20 Shear testing results T/A = 1 (2 mm) (Shear Displacement vs Shear Stress)

4.1.4 Infilled Joints with a Thickness of 3 mm (T/A = 1.5)

Figure 21 shows a comparison of rock joints with an infill thickness of 3 mm (T/A = 1.5) with applied normal stress of 150 kPa, 300 kPa, 450 kPa and 600 kPa. The maximum shear stress values for the tests are lower than previous tests. However, as observed with the infill thickness of 2 mm the reduction in maximum shear stress is less significant as the infill thickness increases. All of the tests show an initial rapid increase in shear stress although as seen in the tests with 2 mm infill thickness the reduction in shear stress after the initial peak is far less than observed previously. The test with a normal stress of 600 kPa shows the wave profile seen earlier, although the variance in the peaks and troughs is far less than in previous tests. The test with a normal stress of 300 kPa doesn't show the wave pattern initially, although, after approximately 10 mm of displacement, the wave pattern emerges. However, the variation in the peaks and troughs is less than in previous tests. As observed with the 2 mm infill thickness tests the shear stress increases throughout the test for all the normal loadings. Unlike previous

infill thicknesses, the test with a normal stress of 150 kPa shows nearly a smooth, gradual increase in shear stress with no visible variance throughout the test as observed previously.

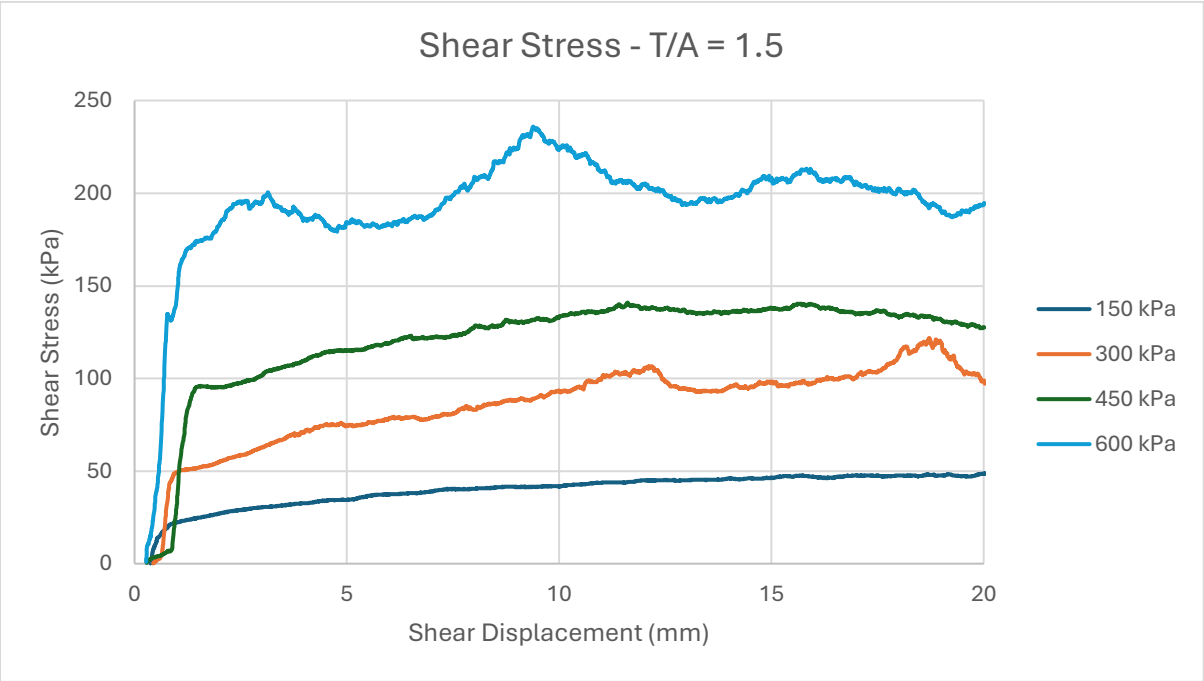

Figure 21 Shear testing results T/A = 1.5 (3 mm) (Shear Displacement vs Shear Stress)

4.1.5 Infilled Joints with a Normal Stress of 150 kPa

Figure 22 shows a comparison of rock joints with a normal stress of 150 kPa with T/A equal to 0, 0.5, 1 and 1.5. The graph shows that all of the samples experienced an initial increase in shear stress with the clean joint sample exhibiting the largest initial increase. As well as this the clean joint showed a wave profile with the wavelength approximately equal to the asperity of the joint. The tests with infill thicknesses of 1 and 2 mm showed some variation after their initial increase in shear stress although they didn't produce a clear wave profile. The test with an infill thickness of 3 mm showed very little variance after the initial increase in shear stress. Although the initial shear stress of the clean joint was far greater than that of the other joints,

the shear stress of all of the joints appears to be trending towards a similar shear stress value of approximately 50 kPa.

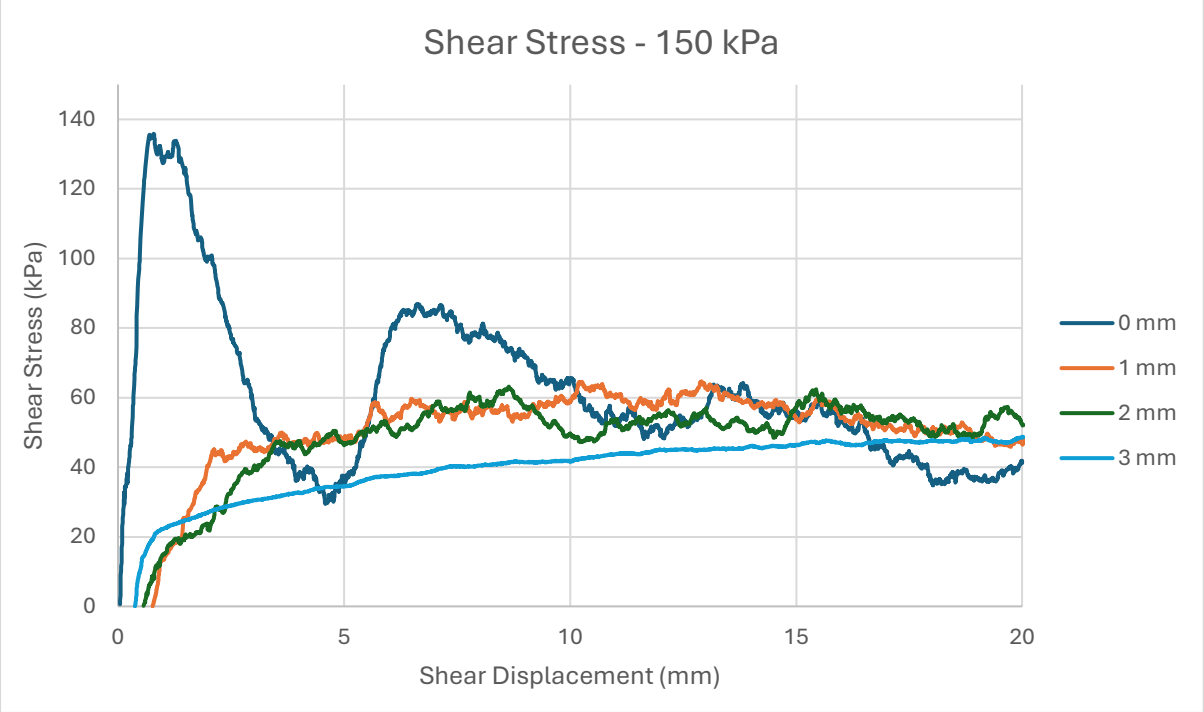

Figure 22 Shear testing results for 150 kPa (Shear Displacement vs Shear Stress)

4.1.6 Infilled Joints with a Normal Stress of 300 kPa

Figure 23 shows a comparison of rock joints with a normal stress of 300 kPa with T/A equal to 0, 0.5, 1 and 1.5. Similar to the graph shown above (Figure 22) the clean joint experiences the greatest initial increase in shear stress followed by a significant decrease. The clean joint once again displayed the wave profile with a wavelength approximately equal to the asperity length of the joint. The tests with infill material included showed similar shear stress values, although, the increase in infill material thickness did slightly decrease the shear resistance of

the joint. As above the shear stress of all of the tests appears to trend towards a shear stress value, of approximately 120 kPa.

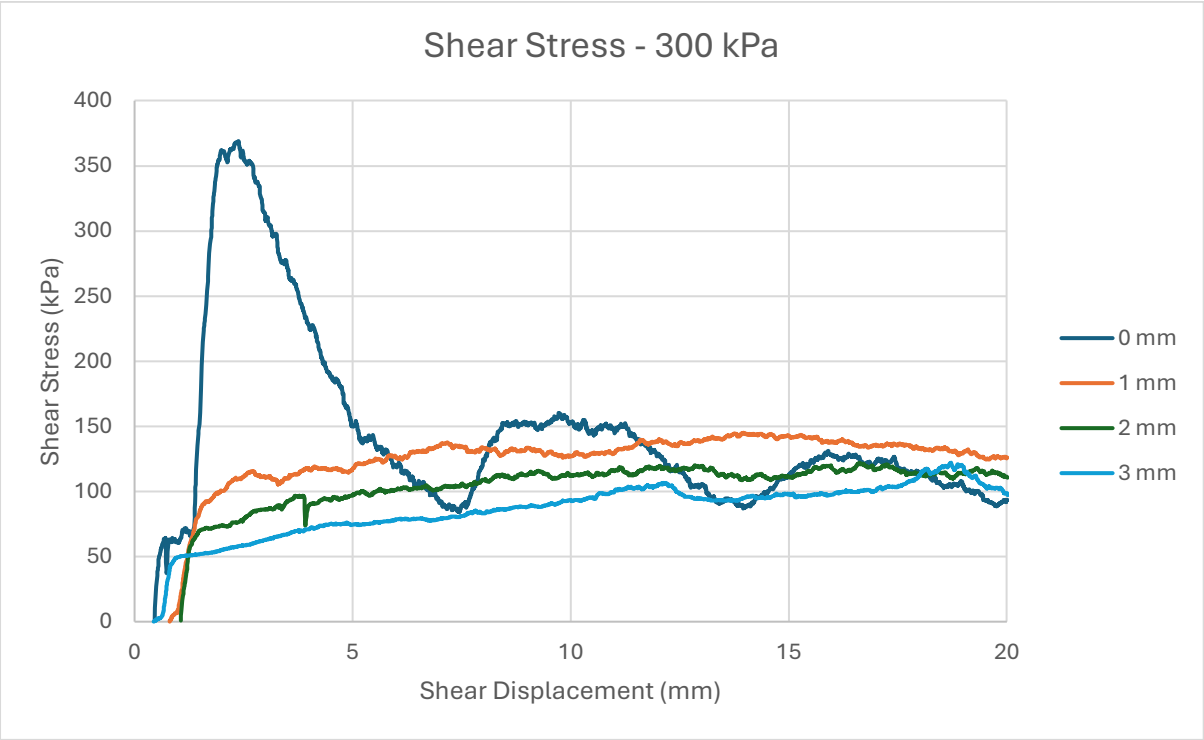

Figure 23 Shear testing results for 300 kPa (Shear Displacement vs Shear Stress)

4.1.7 Infilled Joints with a Normal Stress of 450 kPa

Figure 24 shows a comparison of rock joints with a normal stress of 450 kPa with T/A equal to 0, 0.5, 1 and 1.5. As seen above in Figures 22 and 23, the shear stress rises rapidly in the initial part of the test. For the tests with a clean joint and 1 mm of infill material, the shear stress forms a wave profile after the initial peak in shear stress. This differs from the tests with lower normal stress values as previously the 1 mm infill thickness test hasn't formed a wave profile. The shear stress of the different tests also shows a greater range than previously observed, although as the displacement increases the tests still appear to be converging towards

a shear stress value of approximately 175 kPa. This larger variance in shear stress for the different infill thicknesses implies that as the normal stress is increasing the effect of the infill material on the shear resistance of the joint is reduced.

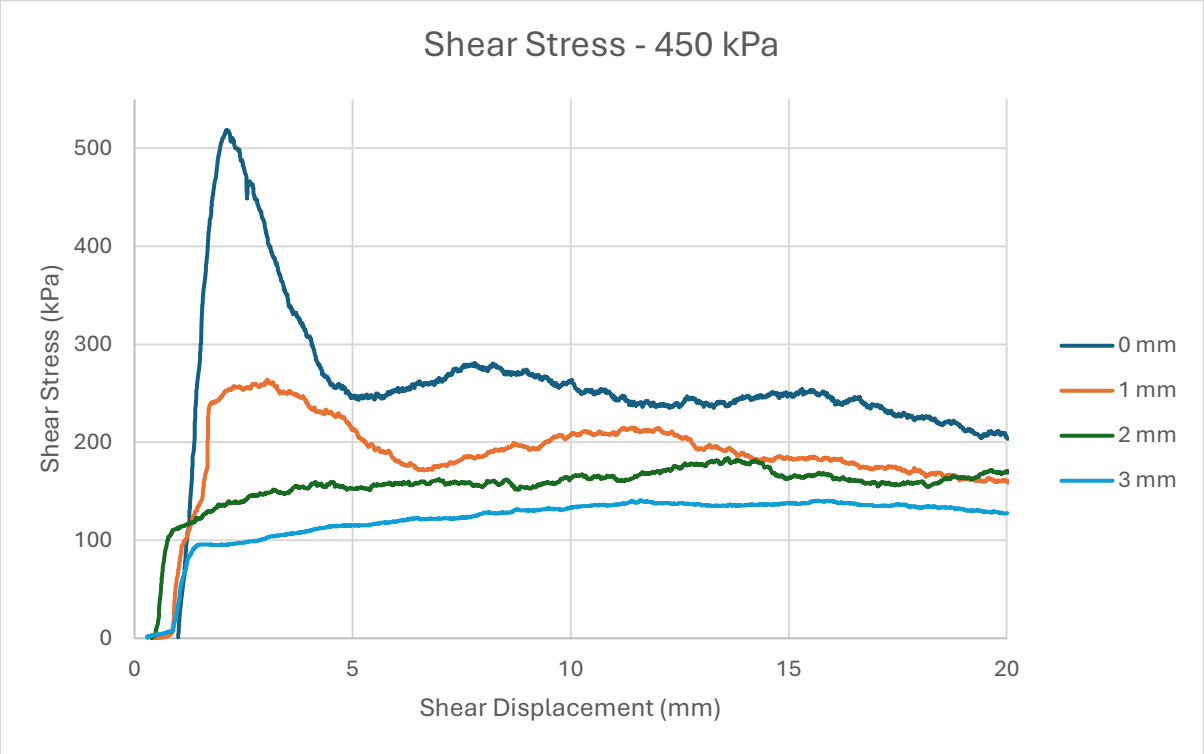

Figure 24 Shear testing results for 450 kPa (Shear Displacement vs Shear Stress)

4.1.8 Infilled Joints with a Normal Stress of 600 kPa

Figure 25 shows a comparison of rock joints with a normal stress of 600 kPa with T/A equal to 0, 0.5, 1 and 1.5. The test with a clean joint was aborted after the shear stress reached the allowable limit of the machine. As observed in previous graphs the shear stress of all of the tests increased rapidly in the initial stages of the test. It can be assumed that had the clean joint test been able to complete the shear stress would have formed a wave profile after the initial shearing of the asperity of the joint. The shear stress of all of the tests with infill material was

again larger than observed in previous graphs. In this graph, the tests with infill thicknesses of 2 mm and 3 mm showed very similar shear stress values and also showed a small wave profile that had not been seen with lower normal stress values. The test with an infill thickness of 1 mm showed a slight wave profile, although, it was not as pronounced as previous graphs. The tests with infill thicknesses of 2mm and 3 mm appear to be converging at a shear stress value of approximately 200 kPa whilst the test with an infill thickness of 1 mm appears to be converging at a shear stress of approximately 300 kPa. This implies that the infill ratio of 0.5 is not the limiting factor for the maximum shear resistance of the joint when the normal loading is 200 kPa. An infill ratio of 1 and 1.5 shows that the limiting factor for the shear resistance of the joint is the shear resistance of the infill material.

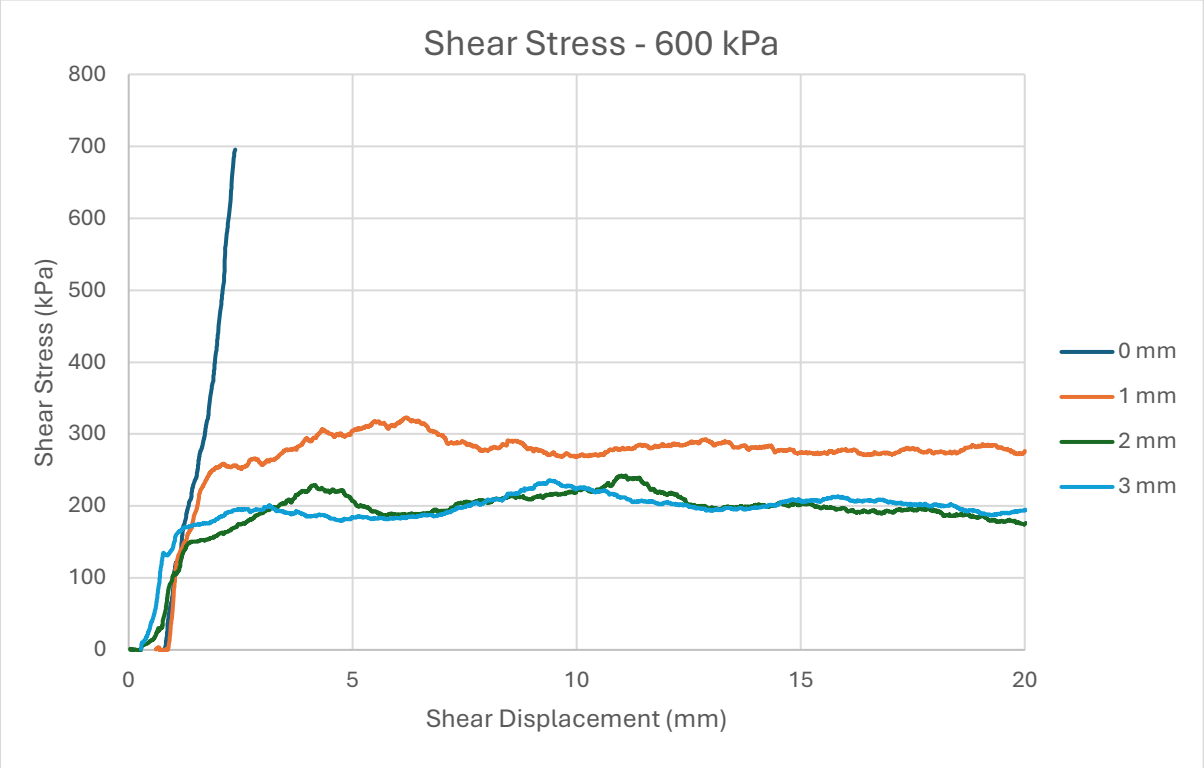

Figure 25 Shear testing results for 600 kPa (Shear Displacement vs Shear Stress)

4.1.9 Summary Shear Displacement VS Shear Stress

The results obtained from the shear testing of rock joints align with the anticipated findings from prior research. When the shear stress of the joint was graphed against the horizontal displacement the results followed a wave pattern with peaks and troughs at approximately 7mm in wavelength matching the asperity length of the rock joint. The wave pattern was most obvious when the infill thickness ratio (T/A) was smaller, as the infill thickness increased, less variation in the shear stress was observed.

The wave profile was most prominent in the clean joint tests, with infilled joints displaying the wave profile at larger normal loadings. Normal stress loadings of 300 kPa or less didn't form a wave profile with infill material present in the joint. The T/A limit for 450 kPa normal stress was 0.5 (1 mm) of infill material whilst the tests with a normal stress of 600 kPa showed the wave profile for all infill thicknesses up to T/A of 1.5 (3 mm). This indicates that for a normal stress of 450 kPa or less, the limiting factor for the shear resistance of the joint is the infill thickness ratio of the joint. Joints with a normal stress of 300 kPa or less have a limiting T/A ratio of less than 0.5 (further testing is required to determine the limiting thickness ratio for these loadings) and for a normal stress of 450 kPa the limiting T/A ratio is 0.5. It must be noted that although the infill thickness of the joint may not be the limiting factor for the shear resistance of the joint, the increase in infill material thickness caused a reduction in the peak and average shear resistance of the joint. From the limited testing and data obtained from this study, it is difficult to determine the exact reduction in shear stress caused by an increase in infill material thickness.

4.2 Shear Displacement vs Normal Stress

This section presents the graphical summaries of the results from the direct shear testing of both clean and infilled rock joints regarding the shear displacement and normal stress variables. The data was collected as outlined above in the methodology with the bulk data processed using Excel.

4.2.1 Infilled Joints with a Normal Stress of 150 kPa

Figure 26 shows a comparison of rock joints with a normal stress of 150 kPa with T/A equal to 0, 0.5, 1 and 1.5. The normal stress reflects a wave profile as was displayed for the shear stress of the rock joints. Once again, the clean joint shows the greatest variance in the peaks and troughs of the waves with the wave profile remaining prominent throughout the test. The test with an infill thickness of 1 mm shows an initial decrease in normal stress (in contrast to the clean joint which showed an increase in normal stress) followed by only minor variations in the normal stress. The tests with an infill thickness of 2 mm and 3 mm showed only minor variations in normal stress throughout the test with no large variations in normal in comparison to the other tests. The test with an infill thickness of 3 mm and 1 mm showed large down-spikes in normal stress at shear displacements of approximately 8.5 mm and 20 mm respectively. These data points can be ignored as they appear as outliers in the data.

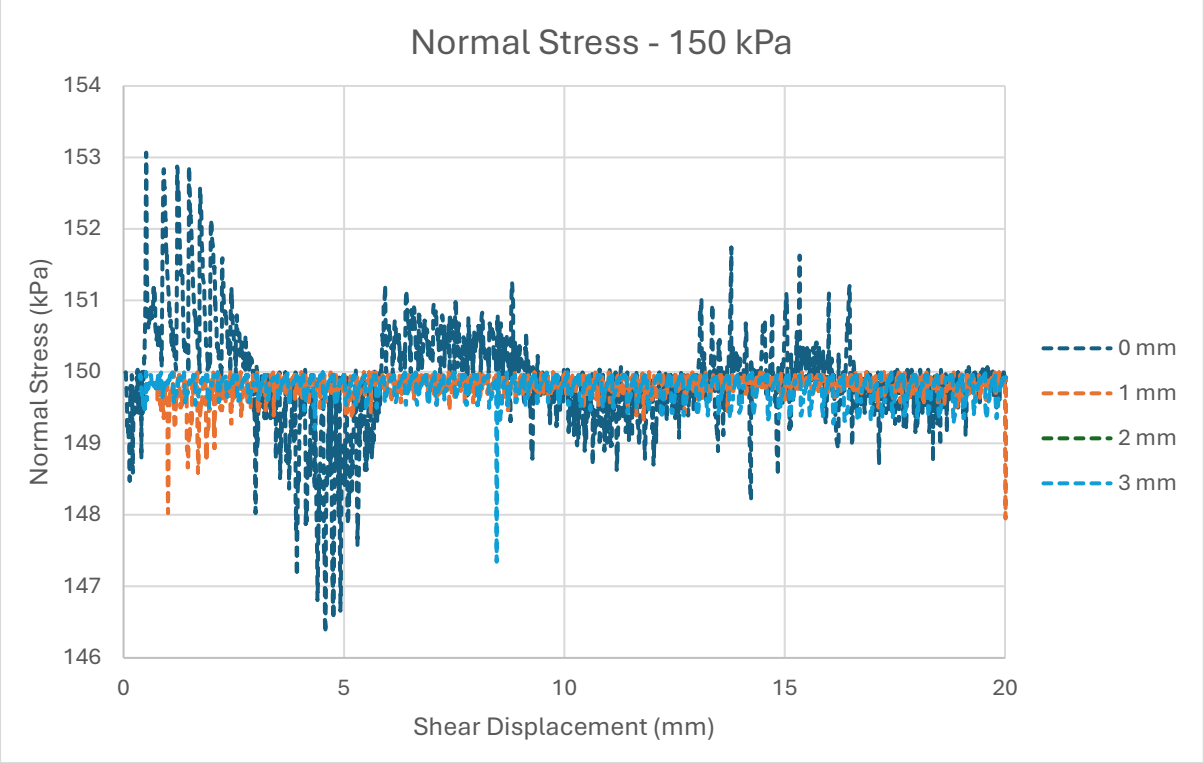

Figure 26 Shear testing results for 150 kPa (Shear Displacement vs Normal Stress)

4.2.2 Infilled Joints with a Normal Stress of 300 kPa

Figure 27 shows a comparison of rock joints with a normal stress of 300 kPa with T/A equal to 0, 0.5, 1 and 1.5. The normal stress of the clean rock joint shows a significant decrease in normal stress at a shear displacement of approximately 0.75 mm of shear displacement. Following this, the normal stress rises and forms a wave pattern with a wavelength of approximately 7 mm. The test with an infill thickness of 1 mm also shows a significant decrease in normal stress at a shear displacement of approximately 1 mm. Following this initial decrease, there is minimal variation in normal stress for the remainder of the test. The test with an infill thickness of 2 mm sees a large down-spike in normal stress at a displacement of approximately 4 mm, this is an outlier in the data and can be ignored for this report. The tests with infill material show minimal variation in the normal stress of the joint throughout the test.

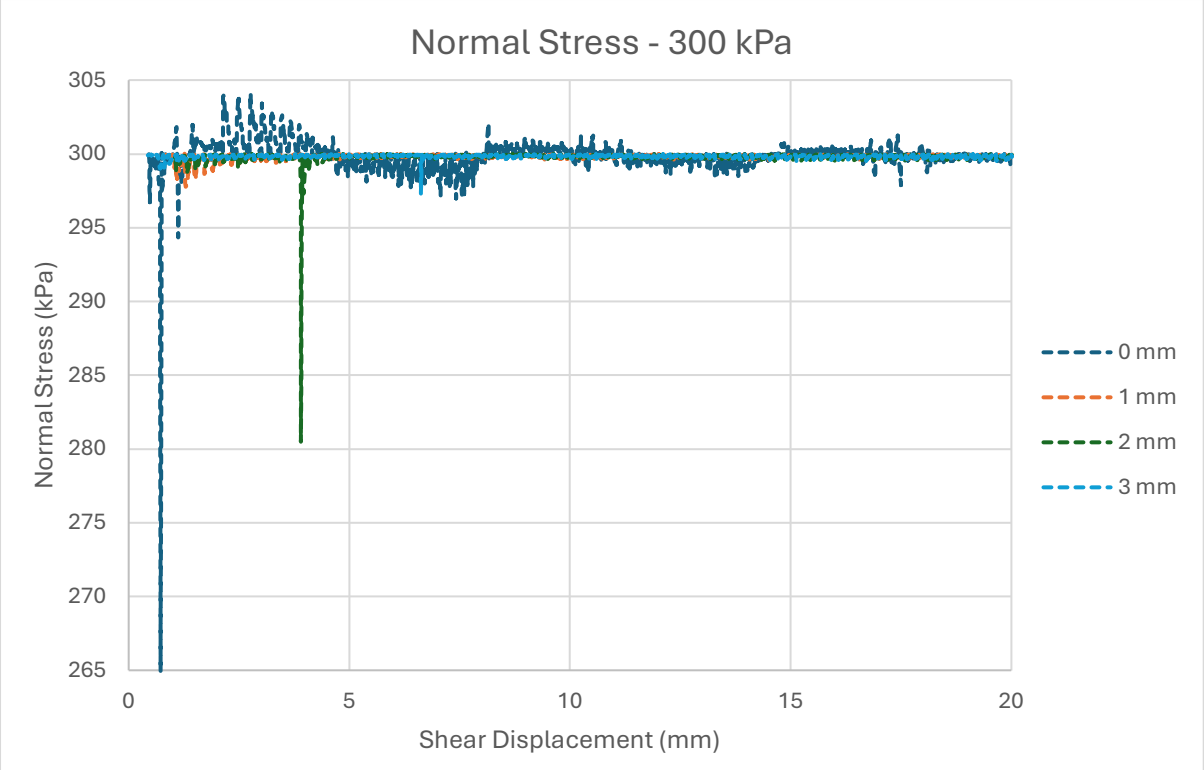

Figure 27 Shear testing results for 300 kPa (Shear Displacement vs Normal Stress)

4.2.3 Infilled Joints with a Normal Stress of 450 kPa

Figure 28 shows a comparison of rock joints with a normal stress of 450 kPa with T/A equal to 0, 0.5, 1 and 1.5. The clean joint along with the joints with 1 mm and 2 mm infill thickness all showed large variations in normal stress at the beginning of the test. The test with an infill thickness of 3 mm also showed some variations in normal stress at the beginning of the test although the extent of the variation was far less than the other tests. The clean joint and joint with an infill of 1 mm showed a wave profile throughout the test although the clean joint showed a greater variance than the infilled joint. The wave profile displayed by the clean joint showed less variance than has been observed for previous, lesser normal stress loadings. This is likely due to the asperity profile of the joint breaking and in effect making the joint a smooth joint.

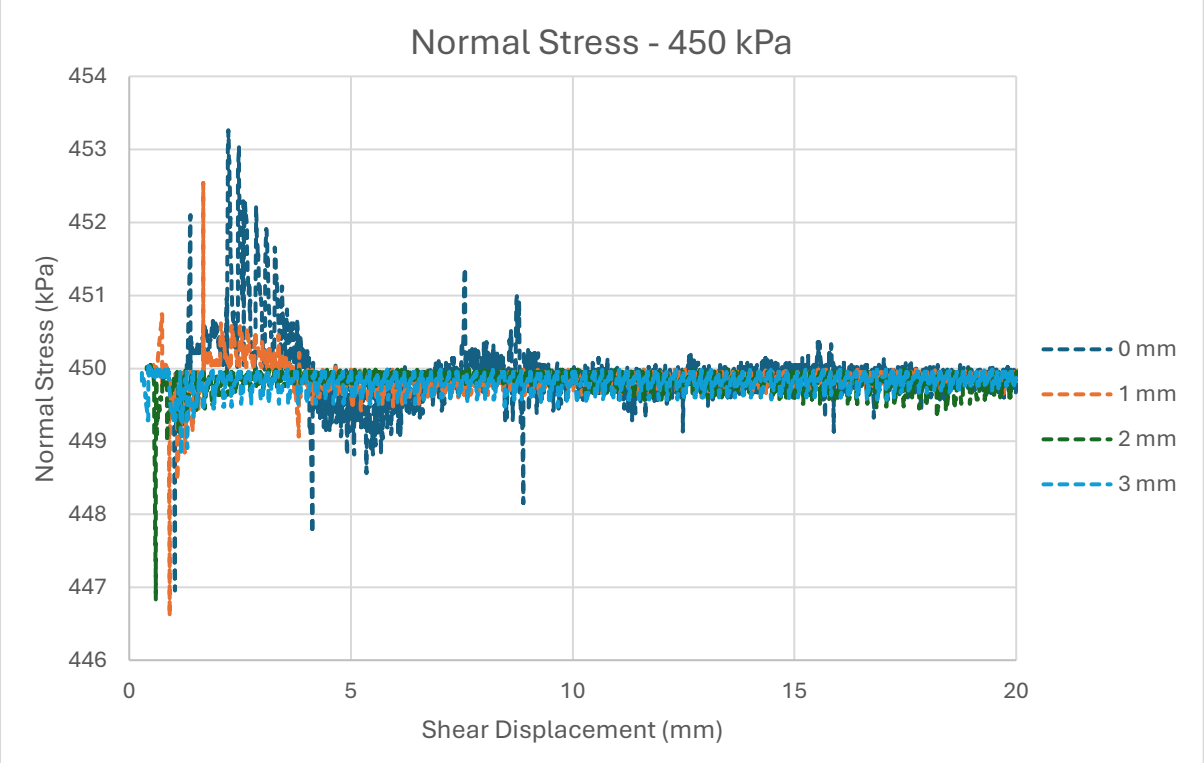

Figure 28 Shear testing results for 450 kPa (Shear Displacement vs Normal Stress)

4.2.4 Infilled Joints with a Normal Stress of 600 kPa

Figure 29 shows a comparison of rock joints with a normal stress of 600 kPa with T/A equal to 0, 0.5, 1 and 1.5. The clean joint test was aborted due to exceeding the limits of the machine. Although, all of the tests showed a significant variation in normal stress at the beginning of the test. The most significant variation was seen in the test with an infill height of 1 mm. The wave profile was also visible in the initial stages of this test, although, it ceased after approximately 7 mm of shear displacement. After 7 mm of displacement, the tests with an infill thickness of 1 mm and 2 mm displayed similar normal stress values. The test with an infill thickness of 3 mm showed similar normal stress values to the 2 mm infill thickness test for the initial 10 mm of shear displacement. Following this, the normal stress in the joint with 3 mm infill material began to reduce for the remainder of the test compared to the other infill joints.

Figure 29 Shear testing results for 450 kPa (Shear Displacement vs Normal Stress)

4.2.5 Summary Shear Displacement VS Normal Stress

A wave pattern is visible in the graphical representations of the shear displacement versus the normal stress for the rock joints, shown above. The wavelength of this pattern is approximately 7 mm, matching the asperity length of the rock joints. The wave pattern is most evident in the clean joints for all of the normal stresses. However, the amplitude of the waves decreases more rapidly with higher normal stress. This indicated that the top portion of the asperity was sheared off with higher normal stress and as a result, the joint became flattened by infilled material.

In comparison, the infilled joints show a larger variation in normal stress throughout the test as the normal stress applied to the sample is increased. The only infill thickness to show the wave pattern is the infill thickness of 1 mm (T/A = 0.5). Although, the wave pattern is only present with a normal stress of 450 kPa and becomes more pronounced with a normal stress of 600 kPa. Again, the reduction in normal stress as the shear displacement increases indicates that

the asperities of the joint were sheared off or infilled with material throughout the test causing the joints to flatten.

5 Conclusion

This research project aimed to investigate the shear behaviour of infilled rock joints under varying normal stress conditions (150 kPa to 600 kPa) for multiple infill material thicknesses (0 mm to 3 mm). The results from the tests conducted without infill material displayed the greatest shear resistance. The introduction of infill material significantly reduced the joint's peak shear resistance, with clean joints displaying a significant initial peak in shear resistance. Conversely, the infilled joints didn't show a defined, significant peak in shear resistance. This indicates that the introduction of infill material allows the joint to slide more freely, preventing significant increases in shear stress as a result of the asperities of the joints contacting and shearing off.

Following the initial peak in shear stress, the average shear resistance of the joints was consistent for all infill material thicknesses. This was most pronounced in tests with lower applied normal stress values of 150 kPa and 300 kPa, as the applied normal stress increased (450 kPa and 600 kPa) a greater variation in shear stress was observed between the different infill material thicknesses. This indicates that the infill material thickness has little bearing on lower shear stresses. In contrast, the higher applied normal stresses compress the infill material more effectively, allowing the asperities of the joint to contact, resulting in increased shear resistance. The wave profile observed in the clean joint tests diminished with thicker infill material thickness. Again, this suggests that the presence of infill material lessens the interaction between the asperities on each rock face.

The study highlights several limitations that would be beneficial for future research. Firstly, time constraints for conducting shear testing resulted in a small sample size and as a result, only 4 infill material thicknesses and loadings were tested. Future studies should include a wider range of infill material thicknesses and loading conditions and consider multiple

moisture contents for the infill material. As well as this the study only used one uniform asperity profile for the joints, a variety of uniform and uniform asperity profiles would be recommended for future research, to better replicate conditions found in naturally occurring rock joints.

6 References

Agustawijaya, D. S. (2007). The Uniaxial Compressive Strength of Soft Rock. *Civil Engineering Dimension* , 9-14.

Asadollahi, P., & Tonon, F. (2010). Constitutive model for rock fractures: Revisiting Barton's empirical model. *Engineering Geology*, 11-32.

Ban, L., Tao, Z., Du, W., & Hou, Y. (2023). A consecutive joint shear strength model considering the 3D roughness of real contact joint surface. *International Journal of Mining Science and Technology*, 617-624.

Bandis, S., Lumsden, A. C., & Barton, N. R. (1981). Experimental studies of the scale effects on the shear behaviour of rock joints. *International Journal of Rock Mechanics and Mining Sciences & Geomechanics Abstracts*, 1-21.

Barton, N. (1976). *The shear strength of rock joints.* Rock Mechanics and Mining Sciences. Retrieved March 2024

Barton, N., & Choubey, V. (1977). *The shear strength of rock joints in theory and practice.* Rock Mechanics and Rock Engineering. Retrieved March 2024

Brekke, T. L., & Howard, T. R. (1972). *Stability problem caused by seems and faults.* Rapid Tunnelling and Excavation Conference.

Crawford, A. M., & Curran, J. H. (1981). The influence of shear velocity on the frictional resistance of rock discontinuities. *International Journal of Rock Mechanics and Mining Sciences & Geomechanics Abstracts*, 505-515.

Downing, E., Mirzaghorbanali, A., & Aziz, N. (2023). *Shear strength properties of clean and clay infilled rock joints: an analysis of the impast of moisture content under CNL conditions of the impast of moisture content under CNL conditions.* Woolongong: University of Wollongong University of Wollongong. Retrieved February 2024

Goodman, R. E. (1976). *Methods of geological engineering in discontinuous rocks.* West Publishing Company.

Heuze, F. E. (1979). Dilatant effects of rock joints. *4th ISRM Congress.* Montreux.

Huang, M., Hong, C., Chen, J., Ma, C., Li, C., & Huang, Y. (2021). *Prediction of Peak Shear Strength of Rock Joints Based on Back-Propagation Neural Network.* International Journal of Geomechanics. Retrieved March 2024

Indraratna, B., Haque, A., & Aziz, N. (1999). Shear behaviour of idealized infilled joints under constant normal stiffness. *Géotechnique*, 331-355.

Indraratna, B., Premadasa, W., Brown, E., Gens, A., & Heitor, A. (2014). *Shear strength of rock joints influenced by compacted infill.* ScienceDirect. Retrieved February 2024

Jaeger, J. C. (1971). *Friction of Rocks and Stability of Rock Slopes.* Geotechnique. Retrieved March 2024

Jafari, M. K., Pellet, F., Boulon, M., & Hosseini, K. A. (2004). Experimental study of mechanical behaviour of rock joints under cyclic loading. *Rock mechanics and rock engineering*, 3-23.

Jahanian, H., & Sadaghiani, M. H. (2014). Experimental Study on the Shear Strength of Sandy Clay Infilled Regular Rough Rock Joints. *Rock Mechanics and Rock Engineering*, 907-922.

Jahanian, H., & Sadaghiani, M. H. (2014). Experimental Study on the Shear Strength of Sandy Clay Infilled Regular Rough Rock Joints. *Rock Mechanics and Rock Engineering*, 907-922.

Jiang, Y., Xiao, J., Tanabashi, Y., & Mizokami, T. (2004). *Development of an automated servo-controlled direct shear apparatus applying a constant normal stiffnesss condition.* International journal of rock mechanics and mining sciences.

Ladanyi, B., & Archambault, G. (1970). Simulation of shear behavior of a jointed rock mass. *Proceedings of the 11th US Rock Mechanics Symposium*, (pp. 105-125). Berkeley.

Ladanyi, B., & Archambault, G. (1977). *Shear strength and deformability of filled indented joints.* International Symposium on Geotechnics of Structurally Complex Formations.

Lama, R. D. (1978). Influence of clay fillings on shear behaviour of joints. *3rd Congr. Int. Eng. Geol.*, (pp. 27-34). Madrid.

Leichnitz, W. (1985). mechanical properties of rock joints. *International Journal of Rock Mechanics and Mining Sciences & Geomechanics Abstracts*, 313-321.

Li, S., Zheng, C., Li, P., & Zhang, S. (2024). Experimental study on I/II/III mixed mode fracture characteristics of a combined rock mass under creep loading. *Scientific Reports*.

Meng, F., Song, J., Yue, Z., Zhou, H., Wang, X., & Wang, Z. (2022). Failure mechanisms and damage evolution of hard rock joints under high stress: Insights from PFC2D modeling. *Engineering Analysis with Boundary Elements*, 394-411.

Naghadehi, M. Z. (2015). *Laboratory Study of the Shear Behaviour of Natural Rough Rock Joints Infilled by Different Soils*. Hamedan University of Technology. Retrieved February 2024

Obert, L., Brady, B. T., & Schmechel, F. W. (1976). *The effect of normal stiffness on the shear resistance of rock*. Rock Mechanics and Rock Engineering.

Ooi, L. H., & Carter, P. J. (1987). *A constant normal stiffness direct shear device for static and cyclic loading*. Geotech Test.

Patton, F. (1966). *Multiple modes of shear failure in rock and related materials*. University of Illinois, Urbana. Retrieved March 2024

Roosta, R. M., Sadaghaiana, M. H., Pak, A., & Saleh, Y. (2006). Rock joint modeling using a visco-plastic. *Geotechnical and Geological Engineering*, 1449-1468.

Sadaghiani, M., & Jahanian, H. (2015). Experimental study on the shear strength of sandy clay infilled regular rough rock joints. *Rock Mech Rock Eng*. Retrieved 03 2024

Saeb, S., & Amadei, B. (1990). *Modelling joint response under constant or variable normal stiffness boundary conditions*. International Journal of Rock Mechanics and Mining Sciences.

Saeb, S., & Amadei, B. (1992). Modelling rock joints under shear and normal loading. *International Journal of Rock Mechanics and Mining Sciences & Geomechanics Abstracts*, 267-278.

Satyarno, I., Solehudin, A. P., Meyarto, C., Hadiyatmoko, D., Muhammad, P., & Afnan, R. (2014). Practical method for mix design of cement-based grout. *2nd International Conference on Sustainable Civil Engineering Structures and Construction Materials 2014 (SCESCM 2014)*, 356-365.

Shrivatava, A. K., & Rao, K. S. (2017, September 18). Physical Modeling of Shear Behavior of Infilled Rock Joints Under CNL and CNS Boundary Conditions. *Rock Mechanics and Rock Engineering*, 101-118. Retrieved March 2024

Suprenant, A. B., & Groom, L. J. (1991). *Designing Grout Mixes*. Detroit: The Aberdeen Group.

Thirukumaran, S., & Indraratna, B. (2016). a review of shear strength models for rock joints subjected to constant normal stiffness. *Journal of Rock Mechanics and Geotechnical Engineering*, 405-414.

Vasarhelyi, B. (1998). *Influence of Normal Load on Joint Dilatation Rate*. Rock Mechanics and Rock Engineering. Retrieved March 2024

Zhao, Y., Zhang, L., Wang, W., Liu, Q., Tang, L., & Cheng, Q. (2020). *Experimental Study on Shear Behavior and a Revised Shear Strength Model for Infilled Rock Joints*. International Journal of Geomechanics. Retrieved February 2024

Zhou, Z., Chen, Z., Shen, Y., Bao, M., Nian, G., Zhang, L., & Liu, Y. (2022). *Failure of Rock Slopes with Intermittent Joints: Failure Process and Stability Calculation Models*. Lithosphere 2022.

Appendix A

Figure 30 Sample A after compression testing

Figure 31 Sample B after compression testing

Figure 32 Sample C after compression testing